

## Dye Removal Form Wastewater Using Efficient and Magnetically Separable Graphene Oxide Composite: Modeling and Optimization Through Response Surface Methodology

<sup>1</sup>Momna Farooq, <sup>1</sup>Muhammad Zahid, <sup>1</sup>Haq Nawaz Bhatti,  
<sup>1</sup>Ijaz Ahmad Bhatti, <sup>2</sup>Asma Rehman and <sup>3</sup>Tajamal Hussain

<sup>1</sup>Department of Chemistry, University of Agriculture, Faisalabad- 38040, Pakistan

<sup>2</sup>National Institute of Biotechnology & Genetic Engineering (NIBGE), Faisalabad, Pakistan

<sup>3</sup>Institute of Chemistry, University of Punjab Lahore, Pakistan

**Abstract:** Graphene oxide (GO) has porous structure with large surface area and can be used as efficient adsorbent. However, its dispersibility and hydrophilic character limits its separation after wastewater treatment with less recyclability. In this study, the magnetic composite of graphene oxide (GO@Fe<sub>3</sub>O<sub>4</sub>) was prepared to ensure easy separation by applying external magnet. The physico-chemical properties of GO@Fe<sub>3</sub>O<sub>4</sub> nanocomposites were characterized by SEM, EDS, XRD and FTIR. The efficiency of GO@Fe<sub>3</sub>O<sub>4</sub> for removing textile reactive dye (Reactive Violet 5R) from wastewater was examined using Response Surface Methodology (RSM). The effect of various parameters such as pH, adsorbent dose, concentration of dye and contact time on the dye removal efficiency was studied. The kinetic study showed that the adsorption of Reactive Violet 5R on GO@Fe<sub>3</sub>O<sub>4</sub> followed pseudo second-order model. The optimization and relationship of different parameters with the removal was investigated by Central Composite Design (CCD) approach. The RSM indicated that pH value of 2.4, adsorbent concentration 206 mg/L, initial dye concentration 42 mg/L and contact time of 94 min were optimized conditions for the maximum 92% removal of Reactive Violet 5R. The CCD proved to be the best statistical model to predict the response with good reliability and precision. The results showed that the GO@Fe<sub>3</sub>O<sub>4</sub> composite proved to be efficient, easily recoverable and stable adsorbent for decontamination of polluted water.

**Key words:** Graphene oxide • Magnetic composite • Textile dyes • Response surface methodology • Wastewater treatment • Organic pollutant

### INTRODUCTION

Recent industrialization is going to be a most serious danger for environment, specially water in developing countries like Pakistan. Where, there is no proper treatment before disposal of effluent into water channels. Textile industries are the major source of lot of pollutants. Faisalabad as an industrial city have 1228 textile units from 6700 reported in Pakistan [1]. High amount of dye releases in water channels during textile processing. About 50% reactive dyes, 20% disperse dye and 2% of basic dyes being unfixed on fabric, are released in wastewater [2, 3]. Dyes have xenobiotic, mutagenic and carcinogenic nature [4]. Dye rich effluent is too dangerous

for living organisms as such dyes absorb sunlight, results decrease in intensity of light to reduce photosynthesis in phytoplankton present in water and also limits oxygenation of water channels [5].

So, it is needed to treat such dye rich wastewater to meet the requirements reusable industrial water. Adsorption is one of the most easily controlled, efficient and has less operating cost among the different techniques including biodegradation, membrane filtration, ozonation and many others [6]. It is important to develop new materials which are highly efficient, having large surface area, selective adsorption of adsorbates, high adsorption rate and easily separable [7, 8]. Carbon based materials are well known adsorbents use for removal of

dyes for many years [9]. Both carbon nanotubes and GO reported to have more potential for adsorption of organic dyes compared to activated carbon [10]. GO is used as adsorbent due to large surface area of 2630 m<sup>2</sup>/g [11]. GO synthesized from graphite by chemical oxidation [12]. Oxidation results in addition of oxygen-containing functional groups like epoxy, hydroxyl and carboxyl groups in graphene yield GO [13]. GO adsorbed organic pollutants by special interactions like  $\pi$ - $\pi$  interaction, hydrogen bonding, van der Waals forces, stacking and electrostatic interactions [14, 15].

Graphene and GO have limitation of restacking and agglomeration of sheets by  $\pi$ - $\pi$  bonding between different sheets, results in loss of surface area and reduces adsorption capacity [16]. The incorporation of nanoparticles like Fe<sub>3</sub>O<sub>4</sub> solve the problem by acting as stabilizing material to prevent aggregation and introduce magnetic character for easy separation. It is difficult to separate GO from water after treatment because of its small size and hydrophilic properties. Magnetic separation needs less energy compared to centrifugation or filtration. Such magnetic particles also have low toxicity, environment friendly and have low cost [10, 17]. The present study planned to investigate the maximum potential of GO@Fe<sub>3</sub>O<sub>4</sub> compared to GO. The Fe<sub>3</sub>O<sub>4</sub> particles may disturb GO sheets and/or reduce its adsorption efficiency. Previous studies reported the effect of different parameters like time, pH, concentration of dye, concentration of adsorbent on adsorption of dyes but did not investigate the interaction between different parameters to affect adsorption. So, in this study we also considered their interaction and optimized such parameters by using Response Surface Methodology. The application of RSM in adsorption process could yield high efficiency, less variability in process, closeness between response and desired requirement, less operating time and cost [18].

## MATERIAL AND METHODS

**Materials:** Graphite powder (98 %), potassium permanganate (KMnO<sub>4</sub>, 99.9%), hydrogen peroxide (H<sub>2</sub>O<sub>2</sub>, 30%), Iron(II) sulfate heptahydrate (FeSO<sub>4</sub>.7H<sub>2</sub>O, 98%), Iron (III) chloride hexahydrate (FeCl<sub>3</sub>. 6H<sub>2</sub>O, 99%) and ammonium hydroxide (NH<sub>4</sub>OH, 30%) were purchased from Daejung, Korea. Sulfuric acid (H<sub>2</sub>SO<sub>4</sub>, 98%), Hydrogen chloride (HCl, 37%) were purchased from Sigma-Aldrich. The chemicals used in this study were of analytical grade.

**Synthesis of Graphene Oxide (GO):** Graphite powder was used to synthesize GO by pressurized oxidation method [19]. In a typical procedure, 2g Graphite, 8g KMnO<sub>4</sub>, 60ml sulphuric acid (98%) and a Teflon chamber were pre-cooled to 0–4 °C in a refrigerator. The teflon chamber was placed in stainless steel autoclave reactor. The cooled graphite and KMnO<sub>4</sub> were put into the chamber and then sulphuric acid was slowly added with gentle stirring. The autoclave reactor was covered and closely tightened after addition of the sulphuric acid. The autoclave was then heated in an oven for 1.5 h to 100 °C. The obtained slurry was diluted with about 1L of water. H<sub>2</sub>O<sub>2</sub> (30%) was added drop wise into it until the slurry turned golden yellow with continuous mechanical stirring. The suspension was sonicated for 1h to get GO from graphitic oxide. The suspension was washed with dilute HCl and then with distilled water till the pH reached 7. The GO was obtained by centrifugation and it was dried in oven at 40°C.

**Preparation of Gomagnetic Composite:** Magnetic composite of GO (Fe<sub>3</sub>O<sub>4</sub>@GO) was synthesized by following the co-precipitation method [20]. Typically, 30 mL of GO (2.7 mg mL<sup>-1</sup>) was ultrasonically dispersed into 80 mL ethanol. Fe<sub>3</sub>O<sub>4</sub> is formed by the co-precipitation of ferrous and ferric ions at the ratio of 1 to 2 in an alkaline medium. The 40 ml solution containing FeCl<sub>3</sub>.6H<sub>2</sub>O and FeSO<sub>4</sub>.7H<sub>2</sub>O was added drop wise into the GO suspension and stirred for 30 min. The mixture was heated to approximately 70°C and ammonia solution was added to adjust the pH to 10. The stirring was continued for 2 h at about 70°C and then cooled down to room temperature. Permanent magnet was used to separate the GO@Fe<sub>3</sub>O<sub>4</sub> composite from the mixture. Magnetic composite was rinsed with distilled water and then with ethanol and dried at 65 °C for 12 h.

**Characterization:** Physical morphology and structure of GO and GO@Fe<sub>3</sub>O<sub>4</sub> magnetic composite were characterized by Scanning electron microscopy (SEM), Fourier transform infrared spectroscopy (FTIR), X-ray powder diffraction (XRD) and Energy-dispersive X-Ray spectroscopy (EDS).

**Adsorption of Reactive Violet 5R on GO and GO@Fe<sub>3</sub>O<sub>4</sub> for Conventional Optimization:** The adsorption of Violet 5R dye from wastewater on GO and GO@Fe<sub>3</sub>O<sub>4</sub> magnetic composite was performed. Different concentrations of

adsorbents were added into Voilet 5R solutions of initial concentrations (10–50 mg L<sup>-1</sup>) under constant stirring. After defined intervals of time, GO was removed from treated dye solution by filtration/centrifugation and GO@ Fe<sub>3</sub>O<sub>4</sub> composite by magnetic separation. Adsorption of Voilet 5R on GO and GO@ Fe<sub>3</sub>O<sub>4</sub> composite was studied within certain conditions such as pH 2–8, time interval (30 min-120min), dye concentration (10-50 mgL<sup>-1</sup>) and concentration of adsorbents (50-250mgL<sup>-1</sup>). The concentration of dye was determined using double beam UV-Visible Spectrophotometer (CECIL CE 7200) at  $\lambda_{\max}$  556nm for Reactive Voilet 5R dye. The percentage removal of dye was evaluated as.

$$\text{Percentage dye removal} = (C_o - C_i) / C_o \times 100 \quad (1)$$

**Process Variables and Experimental Design:** Effect of different parameters on the maximum removal of dye was studied. The parameters included concentration of Reactive Voilet 5R (C<sub>o</sub>), pH of the dye solution, concentration of magnetic composite and time. The Design-expert 9 was used for regression analysis of the experimental data to understand interaction between those independent variables which greatly influence adsorption of dye. A central composite design (CCD) approach of RSM was selected to find out number of experiments for optimization of all operational parameters [21]. Total 21 experiments with eight runs for each of axial and factorial points and five runs for center points were obtained. The center points are so helpful to identify any change in the proposed procedure, as measure of precision (Ravikumar *et al.*, 2005). Lack of fit test, student's t-test and multiple coefficient of determination (R<sup>2</sup>) were performed. Such tests are helpful for the estimation of fitness of model, statistical significance of all estimates and proportion of variance from proposed standards. Batch experimental runs based on CCD were performed to study the interaction between process parameters to affect dye adsorption. The adsorption capacity (mg/g) was evaluated as,

$$q_e = \frac{V(C_o - C_e)}{w} \quad (2)$$

where C<sub>o</sub> is initial and C<sub>e</sub> is equilibrium concentrations (mg/l) of dye present in the test solution, V is solution volume and w is weight of magnetic composite used.

## RESULTS AND DISCUSSION

**Synthesis of GO and GO@Fe<sub>3</sub>O<sub>4</sub>GO:** The GO was obtained from graphite by pressurized oxidation process [19], GO was then dispersed in ethanol by ultrasonication. All oxygen carrying groups act as support for the magnetic nanoparticles. These magnetic particles help to separate the GO sheets apart to prevent aggregation and introduce magnetic character to resulting magnetic composite.

**Characterization:** The synthesized GO was characterized by FTIR and compared its spectra with a sample of GO gifted from **Rune Wendelbo, CEO, Abalonyx, Oslo, Norway**. In Fig 1, FTIR spectra of both samples of GO are same, which confirmed successful synthesis of GO. The bands positioned at 991cm<sup>-1</sup> correspond to stretching mode of epoxy (C-O-C) present on the basal plane of GO. 1617cm<sup>-1</sup> correspond to hydroxyl groups (C-OH) in bending mode; 1721cm<sup>-1</sup> correspond to C=O carbonyl functional group present on edges of GO [22]. 3199cm<sup>-1</sup> correspond to O-H stretching vibrations in hydroxyl and carboxyl groups of GO and residual water present between sheets of GO. The oxygen containing functional groups insert hydrophilic character for high dispersion of GO in water [19]. In Fig. 1 (c), FTIR spectra of GO@Fe<sub>3</sub>O<sub>4</sub> has one peak at 3159 cm<sup>-1</sup> of O-H bond as that in GO. While a new absorption band that appears at about 1096cm<sup>-1</sup> corresponds to deformation vibration of C-O bond. Peak at 1410cm<sup>-1</sup> corresponds to C=C stretching vibration of the GO sheets that ensures the impact of magnetic nanoparticles to restrict the aggregation of GO sheets [7].

SEM image for graphite and exfoliated GO sheet and GO@Fe<sub>3</sub>O<sub>4</sub> are shown in Fig 2. The GO sheets are separated compared to that of graphite and showed layered structure [23]. Oxygen carrying groups including hydroxyl, carboxyl and epoxy helps to stay them apart and increases the overall thickness of GO sheets. In Fig 3. (c, d) it is showed that the Fe<sub>3</sub>O<sub>4</sub> nanoparticles are uniformly distributed on GO sheets. The layered structure of the GO may prevent the Fe<sub>3</sub>O<sub>4</sub> nanoparticles from agglomeration on the same time the Fe<sub>3</sub>O<sub>4</sub> nanoparticles act as a separator between graphene oxide layers. The EDS spectrum in Fig. 2(S) confirmed the presence of C, O and Fe elements in the synthesized GO@Fe<sub>3</sub>O<sub>4</sub> composite. From this analysis, we can deduce that we have successfully introduced the Fe<sub>3</sub>O<sub>4</sub> nanoparticles on GO sheets.

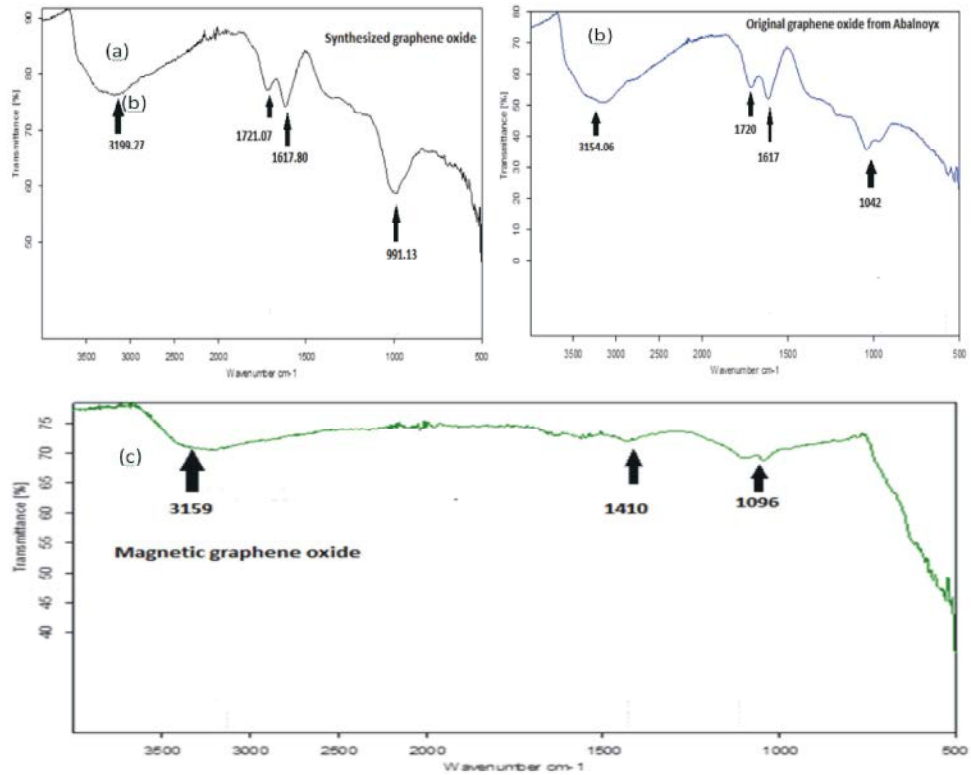


Fig. 1: FTIR spectra of (a) synthesized graphene oxide (b) Original graphene oxide from Abalnoyx (c) GO@Fe<sub>3</sub>O<sub>4</sub>

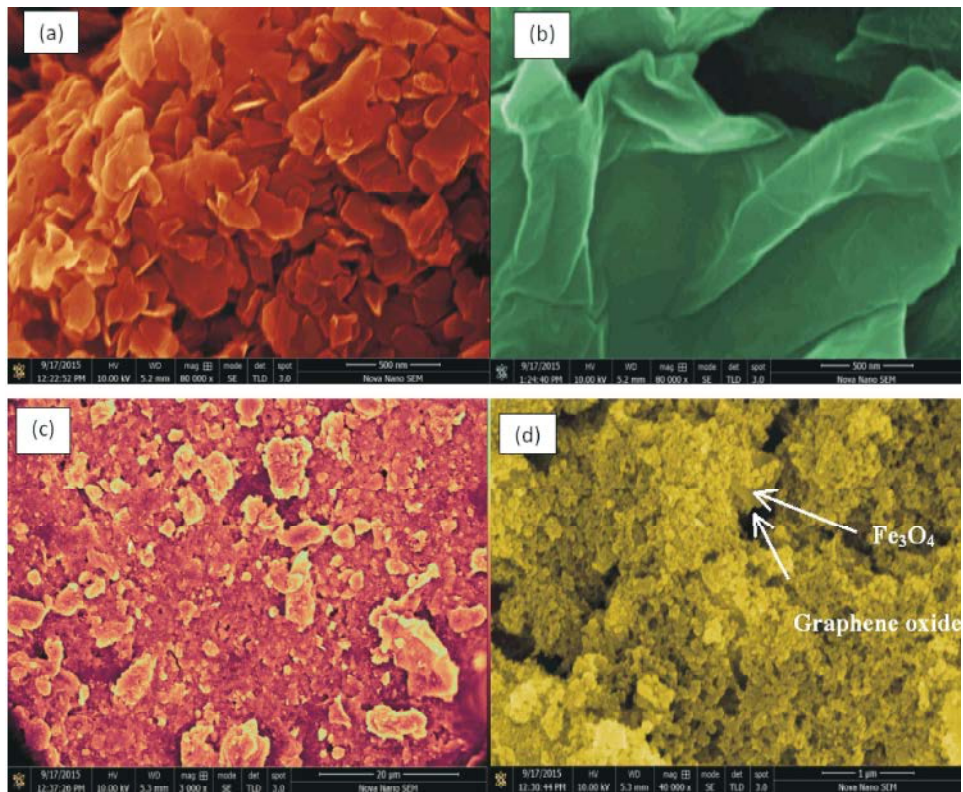


Fig. 2: SEM image of (a) Graphite (b) synthesized graphene oxide (c) (d) GO@Fe<sub>3</sub>O<sub>4</sub>

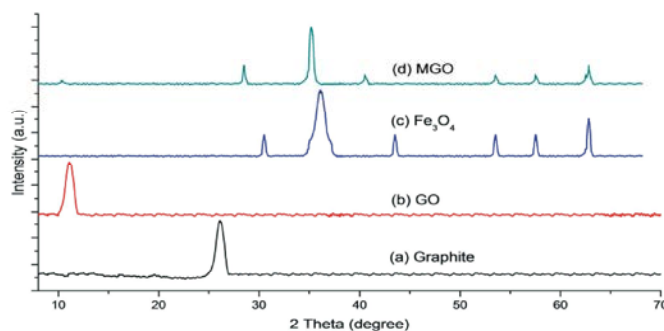


Fig. 3: XRD image of (a) Graphite (b) synthesized graphene oxide (c) Fe<sub>3</sub>O<sub>4</sub> nanoparticles (d) GO@Fe<sub>3</sub>O<sub>4</sub>

XRD patterns of graphite, GO and GO@Fe<sub>3</sub>O<sub>4</sub> have been showed in Fig. 3. The interlayer spacing in graphite has indicated by sharp peak at  $2\theta = 26.1^\circ$ . Fig.3.(b) showed a sharp peak at  $2\theta = 10^\circ$  in GO. Which is clear indication of increase in interlayer distance from 0.32nm present in graphite to 0.8 nm in GO. Oxygen-carrying functional groups like epoxy, carboxyl and hydroxyl are responsible for increase in interlayer distance. Fig. 3 (c) showed XRD patterns of Fe<sub>3</sub>O<sub>4</sub> nanoparticles. The peaks at  $2\theta$  values of  $30.18^\circ$ ,  $35.52^\circ$ ,  $43.36^\circ$ ,  $53.70^\circ$ ,  $57.30^\circ$  and  $62.78^\circ$  are associated with Fe<sub>3</sub>O<sub>4</sub>[20, 23].The results confirmed the presence of magnetic particles of Fe<sub>3</sub>O<sub>4</sub>on the surface of the composite.

### Adsorption Properties

#### Conventional Optimization of Parameters of Adsorption:

Operating parameters, effecting adsorption of dye on GO and GO@Fe<sub>3</sub>O<sub>4</sub> composite are concentration of dye, concentration of adsorbent, pH and contact time.

**Optimization of pH:** Effect of pH on adsorption give several informations about type of interaction occur during adsorption and electrostatic charges are different in acidic or alkaline medium. It is important to select a pH range where adsorbent and pollutants have opposite charges to facilitate ion pairing effect [24]. For this purpose experiments were carried out on pH range 2-8. Zero point charge of graphene oxide and magnetic graphene oxide is reported to be 4.1 and 4.5 [25, 26]. It means the surface of GO and GO@Fe<sub>3</sub>O<sub>4</sub> should be positively charged at pH values lower than zero point charge and negatively charged at pH values higher than zero point charge. A study reported that in acidic medium, Reactive Violet 5R having functional groups  $-\text{SO}_3^-$  and  $-\text{SO}_2\text{CH}_2\text{OSO}_3^-$  as reactive groups which are water soluble. In present study, the adsorption of reactive Violet 5R on GO is favored acidic pH. As shown in Fig. 4 (a) ,90% dye removal reported by GO and 92% by GO@Fe<sub>3</sub>O<sub>4</sub>

at pH 2. Because GO and GO@Fe<sub>3</sub>O<sub>4</sub> has positive charge in acidic medium to attract negatively charged Reactive Violet 5R dye by ion pairing.

**Concentration of Adsorbent:** The adsorption property of GO@Fe<sub>3</sub>O<sub>4</sub> also depends on the van der Waals interactions. There is strong  $\pi$ - $\pi$  stacking interaction between the aromatic ring of dye and the delocalized electron of GO. Presence of such type of strong interfacial interactions (Fe-O-C bonds) between GO and magnetic nanoparticles yield efficient dye removal. In the Fig. 4(b), results showed that adsorption is first increases with increase in concentration of adsorbent and upto a certain concentration. The adsorption of dye at 100mg of GO is due to more number of chemically active sites available at the surface and fast diffusion into the micropores of the GO sheet. This removal have created an increased concentration gradient between dye and adsorbent [27]. At higher concentration, surface area available for adsorption reduced and less dye removed. This may be due to the fact that less number of active sites are exposed and occupied by dye at higher concentration of GO.

**Concentration of Dye:** In the present study, the effect of concentration of dye was investigated by using GO and GO@Fe<sub>3</sub>O<sub>4</sub> with different concentration range (20, 40 and 60mg/L). Fig. 4(c) showed that dye removal increases with the increase in concentration of dye up to 40mg/L. The presence of large number of active sites results in easy diffusion of dye into the pores of GO. Then rapid equilibrium is attained between adsorbent and dye due to attractive forces between sorbent and the adsorbate. This is due to the fast diffusion of dye into inter layered structures. The dye removal decreases in high concentration of the dye due to competition for active sites between molecules of dye.

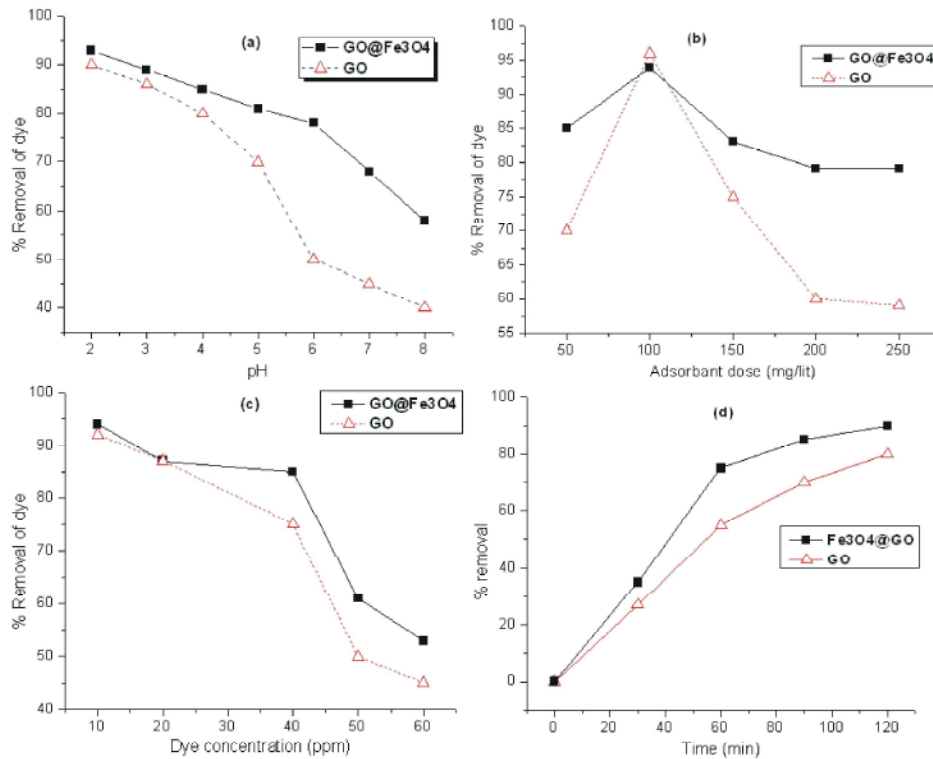


Fig. 4: Effect of experimental parameters (a) pH, (b) adsorbant dose, (c) dye concentration and (d) contact time on the removal of Reactive 5R at different by GO and GO@Fe3O4.

Table 1: Kinetics parameters for adsorption of Reactive Violet 5R on GO and GO@Fe3O4 composite

Adsorbent	Pseudo First order kinetics		Pseudo second order kinetics	
	K <sub>1</sub>	R <sup>2</sup>	K <sub>2</sub>	R <sup>2</sup>
Graphene oxide	0.396	0.54	0.572	0.94
GO@Fe <sub>3</sub> O <sub>4</sub>	0.347	0.44	0.444	0.99

**Contact Time:** It is an important parameter which effects adsorption. The time rangewas selected to be 30- 120 minutes. Results showed that 80% removal of dye reported by GO and 90% by magnetic composite after 120mins as shown in Fig. 4(d). Thisshows higherdye removal efficiency of magnetic graphene oxide.

Adsorption kinetics of the adsorption process gives us information about rate and dynamics of reaction by which conversion of reactants into products possible. Rate of reaction express as increasing rate of products and decreasing rate of reactants. The kinetics of removalof Reactive Violet 5R dye by adsorption is following,

Pseudo-first-order and pseudo-second-order kinetic models were selected to investigate the kinetics of adsorption of Reactive Violet 5R on GO and GO@Fe<sub>3</sub>O<sub>4</sub>magnetic composite.

$$\text{Pseudo-first-order model: } \log (q_e - q_t) = \log q_e - k_1 \frac{t}{2.203} \tag{3}$$

$$\text{Pseudo-second-order model: } \frac{t}{q_t} = \frac{1}{k_2 q_e^2} + \frac{t}{q_e} \tag{4}$$

where q<sub>e</sub> and q<sub>t</sub> are the amounts of Reactive Violet 5R adsorbed (mg g<sup>-1</sup>) at equilibrium and at time t (min), t is the time of adsorption (min), k<sub>1</sub> and k<sub>2</sub> are the pseudo-first and pseudosecond orders rate constants.k<sub>2</sub> find out from the intercept of the plot between t/q<sub>e</sub>and t. The plot of kinetics models (a) Pseudo first order kinetics and (b) Pseudo second order kinetics of removal of dye are shown in Fig. 5. The kinetic constants obtained for boththe models are presented in Table.1. It is observed that adsorption of Reactive Violet 5R on GO and GO/Fe<sub>3</sub>O<sub>4</sub>

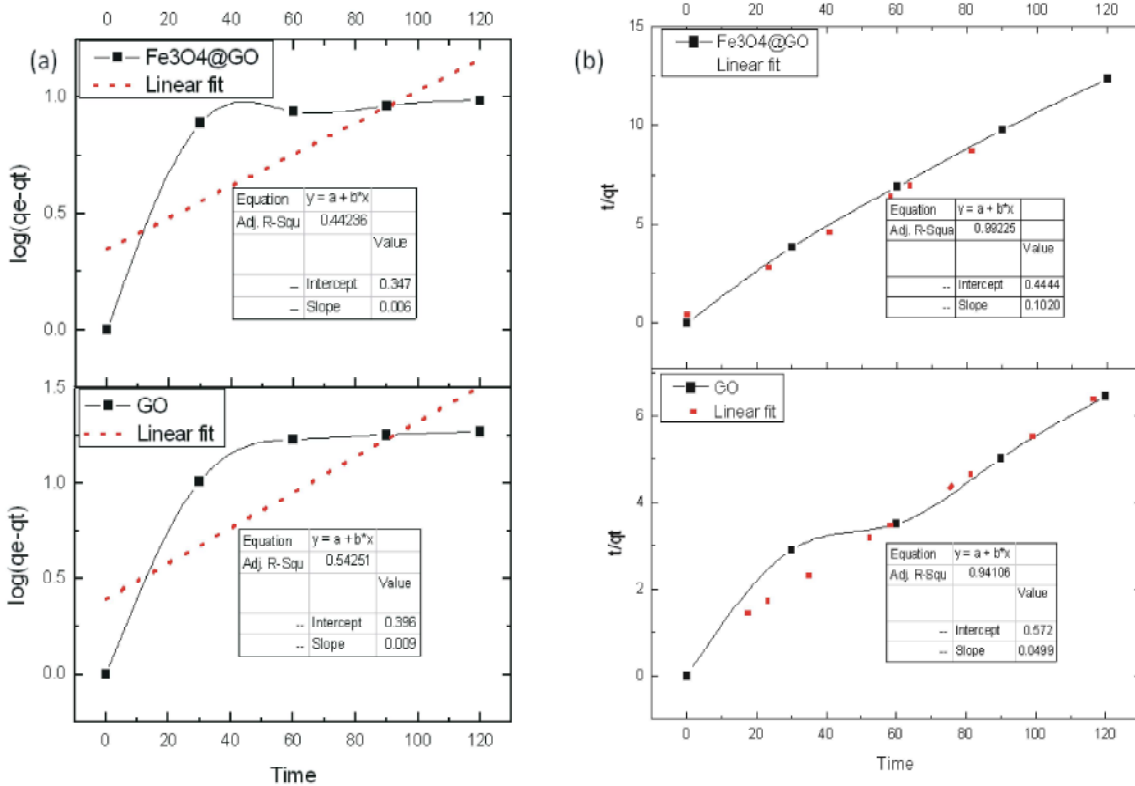


Fig. 5: (a) Pseudo First order kinetics (b) Pseudo second order kinetics of removal of dye by adsorption on GO@Fe<sub>3</sub>O<sub>4</sub> composite.

do not satisfy pseudo first order kinetics. In majority cases, pseudo-first-order model does not fit well to the entire range of contact time, applicable on the initial stages of adsorption [23]. The initial adsorption stage is attained rapidly due to the fast adsorption of the dye molecules on the external surface of the adsorbent. The molecules of dye diffuse slowly into the pores of adsorbent during the later stage because the available external adsorption sites have been already occupied at the initial stage [10]. In case of the pseudo-second-order kinetic model,  $k_2$  depends on the condition of the adsorption like initial dye concentration, pH, temperature, etc. It decreases with the rise in initial concentration of dye, equilibrium will be attained in longer time. The adsorption of Reactive Violet 5R follows the pseudo-second-order kinetics. The results are in accord with the previous research conducting on the removal of rhodamine B and malachite green by Magnetic reduced GO [28] and the removal of methylene blue by GO [29]. Adsorption of dye with GO@Fe<sub>3</sub>O<sub>4</sub> showed that the introduction of Fe<sub>3</sub>O<sub>4</sub> nanoparticles in GO do not disturb its efficiency. In this way we are successfully moved towards efficient, magnetically separable and regenerate able adsorbent.

**Statistical Analysis and Model Fitting:** The experimental design given by CCD model for the removal of Reactive Violet 5R by GO@Fe<sub>3</sub>O<sub>4</sub> is used. The second-order polynomial equation was obtained to check the interaction among various parameters. This equation investigates the empirical relationships between the response and the independent parameters.

$$\begin{aligned} \text{Percentage dye removal} = & +84.92 + 3.29^* A + 20.24^* B - 3.00^* C + 2.16^* D \\ & + 0.019^* AB - 4.48^* AC + 16.04^* AD - 0.39^* BC \\ & + 7.73^* BD + 1.97^* CD - 1.18^* A^2 - 10.22^* B^2 \\ & - 1.07^* C^2 - 0.47^* D^2 \end{aligned}$$

A = pH, B = dye concentration, C = adsorbent dose, D = contact time

ANOVA for Response Surface Quadratic model for magnetic graphene oxide is shown in Table 2. The model terms having probability less than 0.05 are significant. In present model, A (pH), BC (concentration of dye \* concentration of adsorbent), A<sup>2</sup> (pH)<sup>2</sup> and B<sup>2</sup> (concentration of dye)<sup>2</sup> are significant and other terms have values greater than 0.1 are not significant. Fig. 6 shows the comparison between measured and predicted responses of the model and illustrates the accuracy of proposed model. Higher value of R<sup>2</sup> (0.9447) showed that quadratic polynomial expression well predicted the

Table 2: ANOVA for Response Surface Quadratic model for removal of dye by GO@Fe3O4

ANOVA for Response Surface Quadratic model for magnetic graphene oxide						
Analysis of variance table						
Source	Sum of Squares	df	Mean Square	F Value	p-value Prob > F	
Model	4819.16	14	344.23	7.32	0.0111	significant
A-pH	480.50	1	480.50	10.21	0.0187	
B-Concentration of dye	0.000	1	0.000	0.000	1.0000	
C-Concentration of adsorbent	2.58	1	2.58	0.055	0.8226	
D-Contact time	26.40	1	26.40	0.56	0.4821	
AB	26.48	1	26.48	0.56	0.4815	
AC	7.79	1	7.79	0.17	0.6981	
AD	59.49	1	59.49	1.26	0.3038	
BC	390.54	1	390.54	8.30	0.0280	
BD	0.99	1	0.99	0.021	0.8894	
CD	12.24	1	12.24	0.26	0.6282	
A <sup>2</sup>	832.23	1	832.23	17.69	0.0056	
B <sup>2</sup>	2109.82	1	2109.82	44.85	0.0005	
C <sup>2</sup>	68.05	1	68.05	1.45	0.2744	
D <sup>2</sup>	36.97	1	36.97	0.79	0.4095	
Residual	282.26	6	47.04			
Lack of Fit	282.26	2	141.13			
Pure Error	0.000	4	0.000			
Cor Total	5101.42	20				

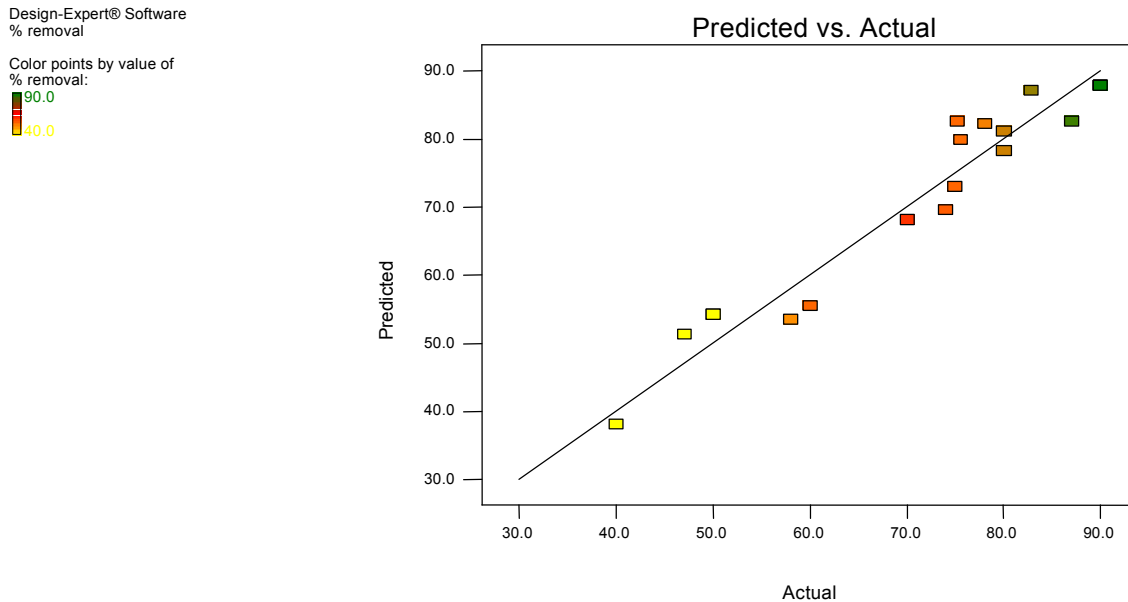


Fig. 6: Experimental values plotted against the predicted values derived from the model designed for removal of dye by GO@Fe3O4 nanocomposite.

removal of reactive Voilet 5R. The value of regression coefficient proved good agreement between actual and observed removal of dye and confirmed the reliability of results.

**Response Surface Analysis:** To investigate the interaction between parameters under their optimum ranges, regression equation give three dimensional

surfaces. Fig. 7(a) showed that the removal of Voilet 5R by GO@Fe<sub>3</sub>O<sub>4</sub> increases with increase concentration of dye upto certain extent and decreases with increase in pH value. This can be featured with the surface charge properties of the adsorbent. In acidic medium, the surface of GO is positively charged. With the rise in pH of the dye solution, negative charge appears on the surface of adsorbent. This decreases the chance of adsorption of



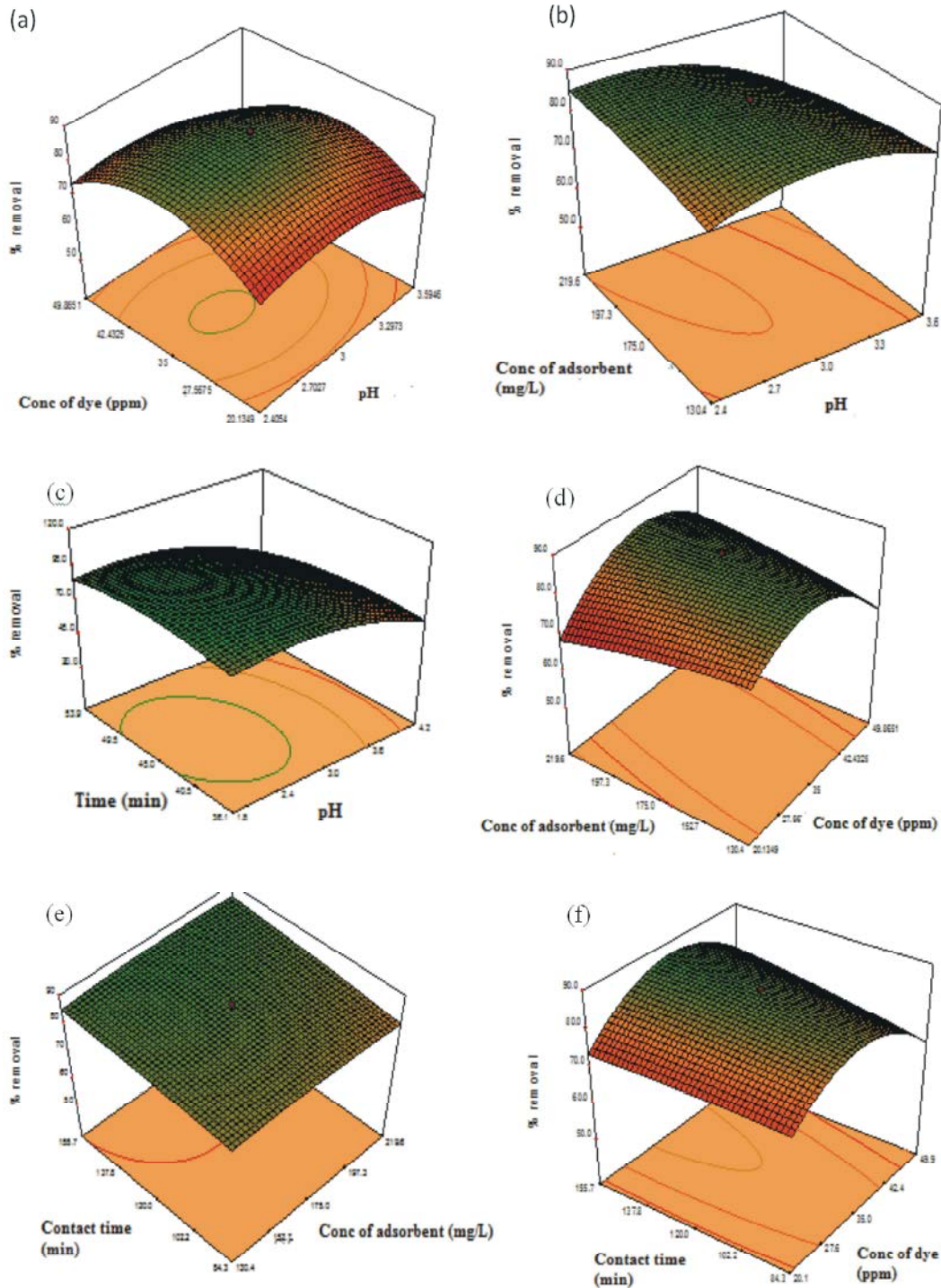


Fig. 7: Interactive effect of different parameters in removal of Reactive Violet 5R dye by GO@Fe<sub>3</sub>O<sub>4</sub> nanocomposite.

dye due to the electrostatic repulsion [30]. With the increase in the concentration of dye their will be a competition between molecules and intermediates of dye for adsorption sites present on the surface of adsorbent.

Fig.7. (b) shows that the removal of dye by GO@Fe<sub>3</sub>O<sub>4</sub> magnetic composite increases with increase in concentration of adsorbent and decrease in pH. At high dose of adsorbent, more surface area is available for

adsorption of dye. In acidic medium the surface charge of adsorbent is more attractive for the adsorption of oppositely charged dye [31]. The removal of dye decreases at large concentration of adsorbent. Due to more saturated the surface area of adsorbent less will be the surface area available for adsorption. Fig. 7.(c) shows that removal of dye by GO@Fe<sub>3</sub>O<sub>4</sub> is increased by the increase in pH upto certain extend. The removal of dye also increases by increasing contact time between dye and adsorbent. Large contact time ensures more adsorption of dye molecules on the surface of adsorbent.

Fig. 7. (d) shows that removal of dye by GO@Fe<sub>3</sub>O<sub>4</sub> decreases with increase in concentration of adsorbent and concentration of dye. At low concentration of dye, the removal of dye faster compared to high dye concentration. With the increase in dye concentration, active sites on adsorbent surface are covered by dye molecules give tough time to other dye molecules. Intermediates of dye also interferes the process of adsorption. With the increase in dye concentration, more dye molecules occupied on active sites and more intermediates of dye are generated but the number of active sites present on adsorbent decreases to occupy them [32]. This phenomena is more influencing at high concentration of dye [32, 33]. For more concentrated solution of dye, more time need to attained maximum removal of dye.

Fig. 7. (e) shows that removal increases by increase in concentration of adsorbent and time upto certain extend. Fig. 7. (f) shows that removal increase by increase in time of contact and decrease in concentration of dye. At less adsorbent dose, more contact time need to achieve high dye removal and for high adsorbent dose less time needed. The dye removal increased with contact time. At high adsorbent dose, large surface area is available for adsorption of dye. Long contact time enhances interaction between the adsorbent and dye to achieve high removal. At low contact time, large surface area and fresh pores of adsorbent are available for adsorption therefore the dye removal was rapid at initial contact time. Than pores of adsorbent filled with adsorbate, have no more pores for extra dye molecule [31].

Adequacy of the proposed model for predicting the maximum removal of Reactive Violet 5R, an experiment was run by using the optimum conditions. An average maximum dye removal of 90% was achieved. Good approximation between the predicted and experimental value confirm the validity of the proposed model.

## CONCLUSIONS

GO@Fe<sub>3</sub>O<sub>4</sub> magnetic composite synthesized by using co-precipitation method proved to be efficient adsorbent. This is a comparative study which confirmed the non-interrupting role of Fe<sub>3</sub>O<sub>4</sub> nanoparticles towards the layered structure of GO. All the results suggested that magnetic property of magnetic nanoparticles in GO@Fe<sub>3</sub>O<sub>4</sub> made it an efficient adsorbent to remove dye. Under the optimized conditions, pH value of 2.4, an initial dye concentration of 42 mg/L, an adsorbent concentration of 206mg/L and contact time of 94min, the removal of Reactive Violet 5R approaches 92%. Regression analysis with R<sup>2</sup> value of 0.94 showed a good agreement between the experimental results and the predicted value.

## ACKNOWLEDGMENTS

The authors are thankful to Mr. RuneWendelbo, CEO, Abalonyx, Oslo, Norway for the GO sample being used for the comparative studies during the stated research. The author(s) acknowledge the support from TWAS under Grant No. 15-410 RG/MSN/AS\_C – FR3240288961.

## REFERENCES

1. Sial, R., *et al.*, 2006. Quality of effluents from Hattar industrial estate. *Journal of Zhejiang University SCIENCE B*, 7(12): 974-980.
2. Tan, N., *et al.*, 2000. Degradation of azo dye Mordant Yellow 10 in a sequential anaerobic and bioaugmented aerobic bioreactor. *Water Science and Technology*, 42(5-6): 337-344.
3. Boer, C.G., *et al.*, 2004. Decolorization of synthetic dyes by solid state cultures of *Lentinula (Lentinus) edodes* producing manganese peroxidase as the main ligninolytic enzyme. *Bioresource Technology*, 94(2): 107-112.
4. Daneshvar, N., *et al.*, Biological decolorization of dye solution containing Malachite Green by microalgae *Cosmarium sp.* *Bioresource Technology*, 2007. 98(6): p. 1176-1182.
5. Dafale, N., *et al.*, 201. Selection of indicator bacteria based on screening of 16S rDNA metagenomic library from a two-stage anoxic-oxic bioreactor system degrading azo dyes. *Bioresource Technology*, 101(2): 476-484.

6. Yao, Y., *et al.*, 2010. Adsorption behavior of methylene blue on carbon nanotubes. *Bioresource Technology*, 101(9): 3040-3046.
7. Zhou, C., *et al.*, 2014. Preparation of Fe<sub>3</sub>O<sub>4</sub>-embedded graphene oxide for removal of methylene blue. *Arabian Journal for Science and Engineering*, 39(9): 6679-6685.
8. Hao, Y., *et al.*, 2015. Kinetics and thermodynamics of diquat removal from water using magnetic graphene oxide nanocomposite. *The Canadian Journal of Chemical Engineering*, 93(10): 1713-1720.
9. Méndez, A., F. Fernández and G. Gascó, 2007. Removal of malachite green using carbon-based adsorbents. *Desalination*, 206(1): 147-153.
10. Li, Y., *et al.*, 2013. Comparative study of methylene blue dye adsorption onto activated carbon, graphene oxide and carbon nanotubes. *Chemical Engineering Research and Design*, 91(2): 361-368.
11. Loh, K.P., *et al.*, 2010. The chemistry of graphene. *Journal of Materials Chemistry*, 20(12): 2277-2289.
12. Liu, J., *et al.*, 2010. Self-Assembling TiO<sub>2</sub> Nanorods on Large Graphene Oxide Sheets at a Two-Phase Interface and Their Anti-Recombination in Photocatalytic Applications. *Advanced Functional Materials*, 20(23): 4175-4181.
13. Haubner, K., *et al.*, 2011. The route to functional graphene oxide. *Chem. Phys. Chem.*, 11(10): 2131-2139.
14. Pyrzynska, K., 2011. Carbon nanotubes as sorbents in the analysis of pesticides. *Chemosphere*, 83(11): 1407-1413.
15. Yang, S.T., *et al.*, 2011. Removal of methylene blue from aqueous solution by graphene oxide. *Journal of Colloid and Interface Science*, 359(1): 24-29.
16. Wu, Z.S., *et al.*, 2010. Anchoring hydrous RuO<sub>2</sub> on graphene sheets for high-performance electrochemical capacitors. *Advanced Functional Materials*, 20(20): 3595-3602.
17. Zhang, W., *et al.*, 2011. Fast and Considerable Adsorption of Methylene Blue Dye onto Graphene Oxide. *Bulletin of Environmental Contamination and Toxicology*, 87(1): 86-90.
18. Annadurai, G., R.S. Juang and D.J. Lee, 2002. Factorial design analysis for adsorption of dye on activated carbon beads incorporated with calcium alginate. *Advances in Environmental Research*, 6(2): 191-198.
19. Bao, C., *et al.*, 2012. Preparation of graphene by pressurized oxidation and multiplex reduction and its polymer nanocomposites by masterbatch-based melt blending. *Journal of Materials Chemistry*, 22(13): 6088-6096.
20. He, G., *et al.*, 2013. Fe<sub>3</sub>O<sub>4</sub>@graphene oxide composite: A magnetically separable and efficient catalyst for the reduction of nitroarenes. *Materials Research Bulletin*, 48(5): 1885-1890.
21. Myers, R.H. and D.C. Montgomery, 1995. *Response Surface Methodology: Process and Product in Optimization Using Designed Experiments*. 1995: John Wiley & Sons, Inc., pp: 728.
22. Fuente, E., *et al.*, 2013. Infrared spectroscopy of carbon materials: a quantum chemical study of model compounds. *The Journal of Physical Chemistry B*, 107(26): 6350-6359.
23. Ai, L., C. Zhang and Z. Chen, 2011. Removal of methylene blue from aqueous solution by a solvothermal-synthesized graphene/magnetite composite. *Journal of Hazardous Materials*, 192(3): 1515-1524.
24. Pavagadhi, S., *et al.*, 2013. Removal of microcystin-LR and microcystin-RR by graphene oxide: Adsorption and kinetic experiments. *Water Research*, 47(13): 4621-4629.
25. Nuengmacha, P., R. Mahachai and S. Chanthai, 2014. Thermodynamic and kinetic study of the intrinsic adsorption capacity of graphene oxide for malachite green removal from aqueous solution. *Oriental Journal of Chemistry*, 30(4): 1463-1474.
26. Hur, J., *et al.*, 2015. Competitive adsorption of metals onto magnetic graphene oxide: comparison with other carbonaceous adsorbents. *The Scientific World Journal*, 2015.
27. Sathishkumar, M., *et al.*, 2007. Two and three-parameter isothermal modeling for liquid-phase sorption of Procion Blue H-B by inactive mycelial biomass of *Panus fulvus*. *Journal of Chemical Technology and Biotechnology*, 82(4): 389-398.
28. Sun, H., L. Cao and L. Lu, 2011. Magnetite/reduced graphene oxide nanocomposites: One step solvothermal synthesis and use as a novel platform for removal of dye pollutants. *Nano Research*, 4(6): 550-562.
29. Li, Y., *et al.*, 2013. Comparative study of methylene blue dye adsorption onto activated carbon, graphene oxide and carbon nanotubes. *Chemical Engineering Research and Design*, 91(2): 361-368.

30. Mohammed, R.R., 2013. Decolorisation of biologically treated palm oil mill effluent (POME) using adsorption technique. *Int Refer. J. Eng. Sci.*, 2(10): 01-11.
31. Alkhatib, M., A.A. Mamun and I. Akbar, 2015. Application of response surface methodology (RSM) for optimization of color removal from POME by granular activated carbon. *International Journal of Environmental Science and Technology*, 12(4): 1295-1302.
32. Khataee, A., *et al.*, 2011. Photocatalytic degradation of an anthraquinone dye on immobilized TiO<sub>2</sub> nanoparticles in a rectangular reactor: Destruction pathway and response surface approach. *Desalination*, 268(1): 126-133.
33. Sleiman, M., *et al.*, 2007. Photocatalytic degradation of azo dye Metanil Yellow: optimization and kinetic modeling using a chemometric approach. *Applied Catalysis B: Environmental*, 77(1): 1-11.